First publ. in: Photochemistry and Photobiology 82 (2006), pp. 495-502

Photochemical Behavior and Na^+,K^+-ATPase Sensitivity of Voltage-sensitive Styrylpyridinium Fluorescent Membrane Probes

Steve Amoroso[1], Vanessa V. Agon[†1], Thomas Starke-Peterkovic[1], Malcolm D. McLeod[1], Hans-Jürgen Apell[2], Pierre Sebban[3] and Ronald J. Clarke[*1]

[1]School of Chemistry, University of Sydney, Sydney, Australia
[2]Fakultät für Biologie, Universität Konstanz, Konstanz, Germany
[3]Laboratoire de Chimie-Physique, Université Paris XI, Orsay, France

ABSTRACT

RH421 is a widely used voltage-sensitive fluorescent membrane probe. Its exposure to continuous illumination with 577 nm light from an Hg lamp leads, however, to an increase in its steady-state fluorescence level when bound to lipid membranes. The increase occurs on the second time scale at typical light intensities and was found to be due to a single-photon excited-state isomerization. Modifications to the dye structure are, therefore, necessary to increase photochemical stability and allow wider application of such dyes in kinetic studies of ion-transporting membrane proteins. The related probe ANNINE 5, which has a rigid polycyclic structure, shows no observable photochemical reaction when bound to DMPC vesicles on irradiation with 436 nm light. The voltage sensitivity of ANNINE 5 was tested with the use of Na^+,K^+-ATPase membrane fragments. As long as ANNINE 5 is excited on the far red edge of its visible absorption band, it shows a similar sensitivity to RH421 in detecting charge-translocating reactions triggered by ATP phosphorylation. Unfortunately the wavelengths necessary for ANNINE 5 excitation are in a region where the Hg lamps routinely used in stopped-flow apparatus have no significant lines available for excitation.

INTRODUCTION

Voltage-sensitive fluorescent styryl dyes, such as RH421, RH160 and di-4- and di-8-ANEPPS, originally developed in the laboratories of Grinvald (1,2) and Loew (3–5), have attracted great interest as a means of optical imaging of electrical field strength within living cells (6,7), visualizing electrical transients in neurons (8–12) and for the investigation of the reaction mechanisms of ion pumps, for example, the Na^+,K^+-ATPase (13–17). In spite of the significant advances that they have no doubt allowed, they do, however, have some drawbacks. The most notable ones are their phototoxicity (18) and their photochemical instability (16,19).

*Corresponding author email: r.clarke@chem.usyd.edu.au
(Ronald J. Clarke)
†Present address: Heart Research Institute, Sydney NSW 2050, Australia

In the course of investigations on the reaction mechanism of the Na^+,K^+-ATPase in which we were using RH421 (see Fig. 1) as a probe to follow the enzyme's partial reactions, we found that the dye underwent a slow photochemical reaction in the second time scale which was characterized by an increase in its fluorescence (16). The reaction of the dye does not significantly interfere with the measurement of the kinetics of reactions associated with the enzyme if they are fast (*i.e.* millisecond time scale) or if the fluorescence change associated with the enzyme reaction is much larger than those associated with the probe. Significant interference does, however, occur if the kinetics of the enzyme-associated reaction is relatively slow, that is, seconds to minutes, or if the fluorescence change of the enzyme-associated reaction is small. The interference can sometimes be minimized by reducing the light intensity with the use of neutral density filters and slowing down the photochemical reaction, but this also has the undesired effect of reducing the signal-to-noise ratio of the enzyme-related signal.

Due in part to these limitations only a very small number of membrane proteins have been kinetically studied with the use of these dyes. The only proteins so far to be investigated include the Na^+,K^+-ATPase (13–17), bacteriorhodopsin (20) and the Ca^{2+}-ATPase (21). The probes are thought to bind predominantly to lipid regions of cell membranes and to detect changes in local electric field caused by charge movement (either transported ions or charged amino-acid residues) associated with ion-binding or release steps or conformational changes of ion pumps (22). These electric field changes would be expected to rapidly decay in strength as one moves laterally away from the protein into the surrounding lipid region. Thus, in order for a probe to show a maximal fluorescence response it should be as close as possible to a charge-transporting membrane protein. This is another major reason why the probes have so far only been used for kinetic studies on the Na^+,K^+-ATPase, bacteriorhodopsin and the Ca^{2+}-ATPase. The very high protein densities of membranes containing these enzymes (approximately 10^3–10^4 per μm^2 [23,24]) means that any probe molecule is not very far away from a protein, and the fluorescence response is, thus, relatively large. If one wished to have voltage-sensitive probes that were applicable to kinetic studies of other ion-transporting membrane proteins that are less densely packed, a number of improvements would be desirable: (1) higher voltage sensitivity; (2) greater photochemical stability; (3) decreased phototoxicity; and (4) higher fluorescence quantum yield. If the photochemical stability could be increased, this would allow measurements to be performed

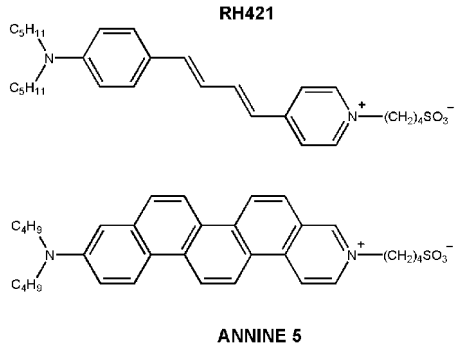

Figure 1. Structures of the fluorescent probes RH421 and ANNINE 5.

at higher incident light intensity with consequent improvements in signal-to-noise ratio. To allow such improvements, however, fundamental studies of the present dyes' photochemical behavior are first required. This is the purpose of the present article.

Recently the group of Fromherz *et al*. (25–27) introduced a new class of voltage-sensitive dyes, the ANNINE dyes. These dyes have anilino and pyridinium rings, like the RH and ANEPPS dyes, but the conjugated double bonds linking the anilino and pyridinium residues are completely bridged by aromatic rings. This would be expected to have major effects on the dyes' photochemical reactions. The aim of this study is, thus, to investigate the photochemical behavior of RH421, one of the most sensitive and widely used of the fast styrylpyridinium dyes, and to compare both its photochemistry and its voltage sensitivity with that of the new dye, ANNINE 5 (see Fig. 1). To test the voltage sensitivity, we will use Na^+,K^+-ATPase membrane fragments, which exhibit significant changes in local intramembrane electric field on phosphorylation of the protein. It should be stressed that it is not an aim of this article to provide any new mechanistic information on the Na^+,K^+-ATPase, but merely use it as a tool for screening dye sensitivity. The eventual aim of our research is to provide a stable dye that can be applied to less-well-studied ion-transporting membrane proteins.

MATERIALS AND METHODS

RH421 was either purchased from Molecular Probes (Eugene, OR) or synthesized by Vanessa V. Agon according to literature methods (1,3). Both samples of dye displayed identical photochemical behavior. With the use of a Bruker (Alexandria, Australia) DPX400 spectrometer (400.20 MHz) the ^{1}H NMR spectrum of the dye was measured in deuterated chloroform. The coupling constants of the olefinic protons were found to be 15 Hz, indicating the E,E (all *trans*) isomeric form, as shown in Fig. 1. ANNINE 5 was a kind gift of Professor Dr. Peter Fromherz, Department of Membrane and Neurophysics, Max Planck Institute for Biochemistry, Martinsried/Munich, Germany. Both dyes were added to either vesicles or Na^+,K^+-ATPase-containing membrane fragments from ethanolic stock solutions. Both dyes are spontaneously incorporated into the membrane.

Na^+,K^+-ATPase-containing membrane fragments were prepared and purified from the red outer medulla of rabbit kidney according to procedure C of Jørgensen (28,29). The specific ATPase activity was measured by the pyruvate kinase/lactate dehydrogenase assay (30), and the protein concentration was determined by the Lowry method (31) with the use of bovine serum albumin as a standard. For the calculation of the molar protein concentration, a molecular weight of an αβ unit of the Na^+,K^+-ATPase of 147 000 g mol^{-1} (32) was assumed. The specific activity of the Na^+,K^+-ATPase preparation used was 734 μmol P_i/mg/h at 37°C. The protein concentration was 3.27 mg/mL.

Dimyristoylphosphatidylcholine (DMPC) was obtained from Avanti Polar Lipids (Alabaster, AL). Unilamellar vesicles were prepared by the ethanol injection method described in detail elsewhere (33,34). The final vesicle suspension contained no detectable trace of ethanol, that is, [ethanol] $\leq$10 μ*M*, according to a nicotinamide adenine dinucleotide/alcohol dehydrogenase enzymatic assay (Boehringer, Mannheim, Germany). All steps of the vesicle preparation were performed at 30°C, that is, above the main phase transition temperature. Dialysis tubing was purchased from Spectrum Laboratories, Inc. (Rancho Dominguez, CA). The phospholipid content of the vesicle suspension was determined by the phospholipid C test from Wako (Osaka, Japan). The vesicles were prepared in a buffer containing 30 m*M* Tris, 1 m*M* EDTA and 150 m*M* NaCl. The pH of the buffer was adjusted to pH 7.2 with HCl.

Photochemical kinetic measurements were carried out with the use of an SF-61 stopped-flow spectrofluorimeter from Hi-Tech Scientific (Salisbury, England). The solution in the observation chamber was excited with a 100 W short-arc mercury lamp (Osram, Munich, Germany), and the fluorescence was detected at right angles to the incident light beam with an R928 multialkali side-on photomultiplier. The exciting light was passed through a grating monochromator with a blaze wavelength of 500 nm. In the case of experiments on RH421, the mercury line at 577 nm was used for excitation, and the fluorescence was collected at wavelengths $\geq$665 nm by using an RG665 glass cutoff filter (Schott, Mainz, Germany) in front of the photomultiplier. For experiments on ANNINE 5, the mercury line at 435 nm was used for excitation, and the fluorescence was collected at wavelengths $\geq$530 nm by using an OG530 glass cutoff filter (Schott) in front of the photomultiplier. Each individual photochemical kinetic measurement was initiated by opening an electromechanical shutter in front of the light source. The kinetic data were collected *via* a high-speed 12-bit analog-to-digital data acquisition board and were analyzed with the use of software developed by Hi-Tech Scientific. Each kinetic trace consisted of 1024 data points. For a typical kinetic measurement over 50 s, this corresponds to a sampling rate of 0.05 s^{-1}. To improve the signal-to-noise ratio, typically between 4 and 10 experimental traces were averaged before the reciprocal relaxation time was evaluated. The error bars shown on the figures correspond to the standard error of a fit of the averaged experimental trace of a set of measurements to a sum (either one or two) of exponential functions. The relaxation time is defined as the time necessary for the difference in fluorescence intensity from its final steady-state value to decay to 1/e of its value at any point in time. Before each experiment the solution in the observation chamber (volume, $V = 2.25 \cdot 10^{-5}$ dm^3) was equilibrated to a temperature of 24°C. The electrical time constant of the fluorescence detection system was set to a value of not less than 10 times faster than the relaxation time of the fastest photochemical transient.

The photon flux of the mercury lamp at 577 nm was determined by potassium ferrioxalate actinometry (35–37). Potassium ferrioxalate $\cdot$ $3H_2O$ was prepared fresh before the measurement by mixing solutions of potassium oxalate $\cdot$ H_2O ($\geq$99.5%, BDH, Kilsyth, Australia) and ferric chloride $\cdot$ $6H_2O$ (99%, BDH), filtering and recrystallizing the resultant potassium ferrioxalate crystals four times from warm water. An aqueous solution of 0.15 *M* potassium ferrioxalate was irradiated for 5 min. The amount of Fe^{2+} formed was determined absorptiometrically after complexation with 1,10-phenanthroline $\cdot$ H_2O (analytical grade, Merck, Kilsyth, Australia). For the determination of the Fe^{2+} formed, a standard curve was constructed by complexation of solutions of various concentrations of ferrous sulphate $\cdot$ $7H_2O$ ($\geq$99.5%, BDH). The value of the quantum yield, q, of Fe^{2+} on photolysis of the potassium ferrioxalate solution was taken to be 0.013 (37). The photon flux, I_O (the number of incident quanta per second) was then calculated according to

$$I_O = \frac{n_{Fe} N_A}{q(1 - 10^{-A_{Fe}})} \cdot \frac{1}{t} \qquad (1)$$

where A_{Fe} is the absorbance of the potassium ferrioxalate solution at 577 nm in the observation chamber of the stopped-flow instrument (path length 1 cm), n_{Fe} is the number of moles of Fe converted, N_A is Avogadro's constant and t is the time of irradiation in seconds.

Absorbance measurements were performed with a Shimadzu (Rydalmere, Australia) UV-2450 UV-visible recording spectrophotometer with the use of a bandwidth of 5 nm. Steady-state fluorescence measurements were recorded with a Shimadzu RF-5301PC spectrofluorophotometer. To minimize contributions from scattering of the exciting light and higher-order wavelengths, glass cut-off filters were used in front of the excitation and emission monochromators. For measurements using DMPC vesicles, the temperature of the cuvette holder was thermostatically controlled to 30°C, that is, above the main phase-transition temperature of 23°C (38), so that the lipid was in its liquid crystalline state. For measurements using

Na^+,K^+-ATPase-containing membrane fragments, the temperature of the cuvette holder was thermostatically controlled to 24°C. All measurements using the Na^+,K^+-ATPase were conducted with the use of a buffer of the following composition: 30 m*M* imidazole, 130 m*M* NaCl, 5 m*M* $MgCl_2$ and 1 m*M* EDTA. The pH of the buffer was adjusted to 7.4 by the addition of HCl. K^+ ions were excluded from the buffer to minimize the rate of enzyme dephosphorylation following the addition of ATP. Phosphorylation of the Na^+,K^+-ATPase (22 μg/mL) membrane fragments labeled with either RH421 or ANNINE 5 (150 n*M*) was initiated by adding 1 m*M* of either MgATP or Na_2ATP directly to the cuvette. This causes a phosphorylation and conformational change of the enzyme, converting it from an initial $E_1(Na^+)_3$ state to a final E_2P state (16,39).

The origins of the various reagents used were as follows: imidazole (99+%, Sigma, Castle Hill, Australia), tris-[(hydroxymethyl)amino]methane (99.9%, Sigma), EDTA (99%, Sigma), NaCl (analytical grade, Merck), $MgCl_2 \cdot 6H_2O$ (analytical grade, Merck), HCl (0.1 *N* Titrisol solution, Merck), ATP magnesium salt $\cdot 5.5H_2O$ (~97%, Sigma), ATP disodium salt $\cdot 3H_2O$ (special quality, Roche, Castle Hill, Australia), methanol (>96%, CSR Ltd, Yarraville, Australia), ethanol (>96%, CSR Ltd), pentanol (99.9%, Ajax Chemicals, Auburn, Australia), hexanol (>98%, Merck), heptanol (>99%, Merck), propanol (≥99.5%, Merck), butanol (≥99%, Merck) and chloroform (≥99.8%, Fluka, Castle Hill, Australia).

THEORY

It is already well established that fluorescent dyes, such as RH421, based on the stilbene structure can undergo *trans* → *cis* and *cis* → *trans* photoisomerization (19). Laser pulse studies have indicated that the equilibrium between *trans* and *cis* configurations in the excited state is established on the time scale of <10 ns (40,41). Is it then at all feasible that such a rapid reaction could interfere with measurements on the Na^+,K^+-ATPase or other ion pumps on the stopped-flow time scale of milliseconds to seconds?

Consider a mechanism whereby a molecule X undergoes excitation, followed by a unimolecular reaction in the excited state and finally deactivation (either *via* fluorescence or radiationless) to a new ground-state species, Y:

$$\mathrm{X} \overset{K}{\leftrightarrow} \mathrm{X}^* \underset{k_{-1}}{\overset{k_1}{\leftrightarrow}} \mathrm{Y}^* \overset{K'}{\leftrightarrow} \mathrm{Y}$$

If, under conditions of continual illumination, the steady state between the excitation and emission reactions of X and Y is reached much faster than the excited-state reaction, X* ↔ Y*, can reach equilibrium, the first and last steps can be considered as rapid equilibria with partition coefficients K and K'. Considering the configurational change alone, one can then simplify the reaction scheme to

$$\sum \mathrm{X} \leftrightarrow \sum \mathrm{Y}$$

where $\sum$X and $\sum$Y represent all of the X and Y species, respectively; that is, X + X* and Y + Y*. The differential rate equation for this reaction scheme is given by

$$-\frac{d\sum \mathrm{X}}{dt} = k_1[\mathrm{X}^*] - k_{-1}[\mathrm{Y}^*] \tag{2}$$

where k_1 and k_{-1} are the forward and backward rate constants for the isomerization reaction in the excited state. The reaction can be initiated by the opening of a shutter, after which the system will relax into a new equilibrium position or steady state at the much higher light intensity. Similar to (Eq. 2), the kinetics of relaxation into the new equilibrium or steady state is given by

$$-\frac{d\Delta\sum \mathrm{X}}{dt} = k_1\Delta[\mathrm{X}^*] - k_{-1}\Delta[\mathrm{Y}^*] \tag{3}$$

where $\Delta\sum$X is the deviation of $\sum$X from its final steady-state value and, similarly, Δ[X*] and Δ[Y*] are the deviations of [X*] and [Y*] from their final steady-state values caused by the opening of the shutter. Because the excitation reactions are assumed to be in equilibrium on the time scale of the excited-state isomerization, it can be shown that Δ[X*] and Δ[Y*] are related to $\Delta\sum$X by

$$\Delta[\mathrm{X}^*] = \frac{K}{1+K} \cdot \Delta\sum \mathrm{X} \tag{4}$$

$$\Delta[\mathrm{Y}^*] = -\frac{K'}{1+K'} \cdot \Delta\sum \mathrm{X} \tag{5}$$

Substituting these two expressions into the differential rate equation (Eq. 3) and integrating yields the following equation for the reciprocal relaxation time:

$$\frac{1}{\tau} = \frac{K\ k_1}{1+K} + \frac{K'k_{-1}}{1+K'} \tag{6}$$

where τ, the relaxation time, is the time necessary for $\Delta\sum$X to drop to $1/e$ of its initial value. The reciprocal relaxation time, $1/\tau$, is also sometimes called the observed rate constant. Equation 6 predicts how the experimentally determined $1/\tau$ value is related to the partition coefficients, K and K', and the rate constants for the individual reactions in the excited state. From (Eq. 6) it can be seen that the value of $1/\tau$ will only be equal to $(k_1 + k_{-1})$, the expected reciprocal relaxation time for the excited-state isomerization, if all of the probe is in the excited state; that is, $K \gg 1$ and $K' \gg 1$. If, as would be expected, under constant illumination the majority of the dye is still in the ground state, that is, $K \ll 1$ and $K' \ll 1$, (Eq. 6) reduces to

$$\frac{1}{\tau} \approx K\ k_1 + K'\ k_{-1} \tag{7}$$

Under these circumstances, the experimentally observed value of $1/\tau$ could be on a much longer time scale than that of the excited-state isomerization.

The values of K or K' are determined by the light intensity, the absorbance of the compound and its rate of deactivation, either *via* fluorescence or radiationless deactivation. Thus, for the species X,

$$K = \frac{[\mathrm{X}^*]}{[\mathrm{X}]} = \frac{I_A}{(\Gamma + k)} = I_A \cdot \tau_F \tag{8}$$

where I_A is the number of quanta absorbed per molecule per unit time, Γ is the rate constant for fluorescence emission, k is the rate constant for radiationless deactivation and $\tau_F (=1/[\Gamma + k])$ is the fluorescence lifetime. An analogous equation can be written for K' and Y. The number of quanta absorbed per molecule per unit time depends both on its absorbance and the incident light intensity, that is, the photon flux, I_O. It is given by the following expression:

$$I_A = I_O \cdot \frac{1 - e^{-2.303A}}{N_A[\mathrm{X}]V} \tag{9}$$

where A is the absorbance of the species X at the wavelength of the incident light, [X] is the molar concentration of X in the observation chamber and V is the volume of the observation chamber (in dm^3). Combining (Eqs. 8 and 9) yields the following final equation for the distribution of X between the ground and excited states:

$$K = \frac{[\mathrm{X}^*]}{[\mathrm{X}]} = I_O \cdot \frac{1 - e^{-2.303A}}{N_A[\mathrm{X}]V} \cdot \tau_F \tag{10}$$

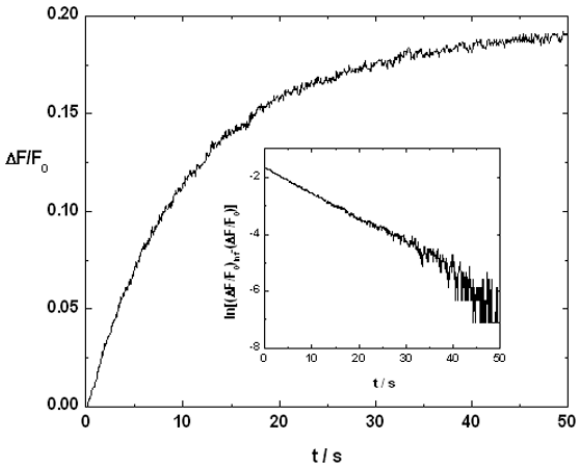

Figure 2. Relative fluorescence intensity, $\Delta F/F_0$, of RH421 bound to DMPC vesicles as a function of time. At $t = 0$, the suspension was exposed to 577 nm light from a mercury arc lamp and the fluorescence emission was recorded at wavelengths $\geq$665 nm; [RH421] = 1.7 μM, [DMPC] = 3 mM, pH = 7.2, $T = 30°C$. The reciprocal relaxation time, $1/\tau$, for this transient was 0.0894 ($\pm$0.0002) s^{-1}. The insert shows the same kinetic trace, but here the relative fluorescence intensity has been converted to $\ln[(\Delta F/F_0)_{inf} - \Delta F/F_0]$, where $(\Delta F/F_0)_{inf}$ represents the relative fluorescence intensity at infinite time. The linear nature of the insert plot indicates that the fluorescence increase follows a single exponential time function.

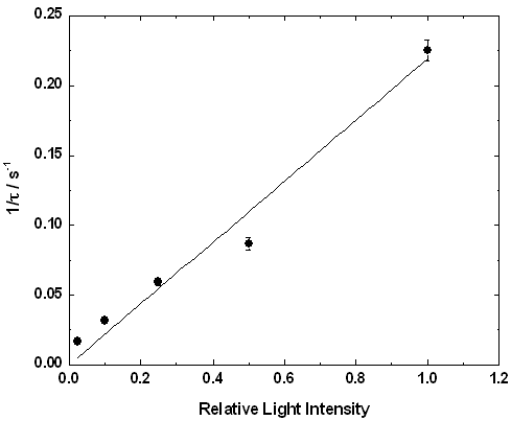

Figure 3. Dependence of the reciprocal relaxation time, $1/\tau$, of the RH421 photochemical reaction on the relative light intensity. The light intensity was adjusted by placing neutral density glass filters (Schott, Mainz, Germany) in the excitation light beam. All other experimental conditions were as given in Fig. 2.

Again an analogous equation could be written for Y and K'. After determining a value for K from (Eq. 10), this can then be combined with experimental data for $1/\tau$ from kinetic data obtained from continuous illumination, so that an estimate of the true rate constant for the isomerization reaction in the excited state, k_1, can be obtained from (Eq. 7).

The reciprocal relaxation time for the establishment of the steady state between the ground and excited states is given by $I_A + 1/\tau_F$. As long as this is much greater than the measured $1/\tau$ after opening of the shutter, the assumption of the derivation that the excitation and emission reactions are in equilibrium and uncoupled from the photoisomerization is justified. If the observed fluorescence change after opening the shutter occurs on the second time scale (as it does for RH421), this condition is well and truly satisfied for any typical dye having a fluorescence lifetime in the nanosecond time range. Experimentally the establishment of the steady state between the ground and excited states is observed on opening the shutter as an unresolvable instantaneous jump in fluorescence, which occurs before the subsequent slow increase in fluorescence.

The derivation of the equation for the dependence of reciprocal relaxation time on the rate constants of the excited-state reaction and the intensity of the incident radiation (Eq. 7) involves the application of relaxation kinetics theory to a photochemical reaction. The treatment is, thus, analogous to that used for describing temperature-jump kinetic data, where a system in equilibrium is rapidly perturbed by a sudden jump in temperature. In our case the perturbation of the system comes about by a sudden increase in light intensity (*via* opening of a shutter), that is, from zero light intensity to constant illumination. The experiment could be referred to as a ''light jump'' experiment. The method and the theoretical treatment of the data are, therefore, quite different from the flash-photolysis technique often applied to photochemical systems, which requires a very intense short light pulse, after which the reaction of the excited-state molecules is directly observed.

RESULTS

Photochemistry of RH421

Irradiation of RH421 bound to DMPC lipid vesicles with 577 nm wavelength light leads to an increase in dye fluorescence over the time scale of seconds (see Fig. 2). The kinetics of the fluorescence increase can be well described by a single exponential time function. If the dye–vesicle suspension is exposed to light for longer periods of time, that is tens of seconds, a fluorescence decrease is subsequently observed, indicating a photobleaching process. The reciprocal relaxation time for the fluorescence increase is independent of both dye and lipid concentration, but it increases linearly with the intensity of the exciting light (see Fig. 3). This indicates that the reaction being observed must be a first-order change in the configuration of membrane-bound dye, which is caused by single-photon absorption.

To test the reversibility of the reaction in the absence of illumination, a dye–vesicle suspension was first irradiated until the initial fluorescence increase was completed. The suspension was then left in the dark for periods of up to 5 min. When the shutter was again opened and the suspension was exposed to light, the same fluorescence level was observed. On this time scale the reaction can thus be considered to be irreversible when the system is not exposed to light. This can easily be understood on the basis of (Eq. 7). In the dark, the fraction of the product Y in an excited state would be expected to be vanishingly small; that is $K' \rightarrow 0$. Therefore, the mechanistic pathway for reversal of the reaction is no longer available. In effect, closing of the shutter hence ''locks in'' the distribution of dye between the X and Y configurations which had been reached during the previous illumination. Furthermore, the lack of dark reversibility is a clear indication that the photochemical reaction being observed must involve the formation of a new ground-state species. It cannot simply be due to a light-induced solvent reorganization around an excited dye molecule, because solvent reorganization requires no significant energy input and the solvent ''cage'' would be expected to revert rapidly (on the picosecond time scale) in the dark to its original conformation (42). Similarly, the reaction cannot be attributed to the formation of an excited twisted intramolecular charge transfer (TICT) state, which involves twisting around a single bond, because this also requires

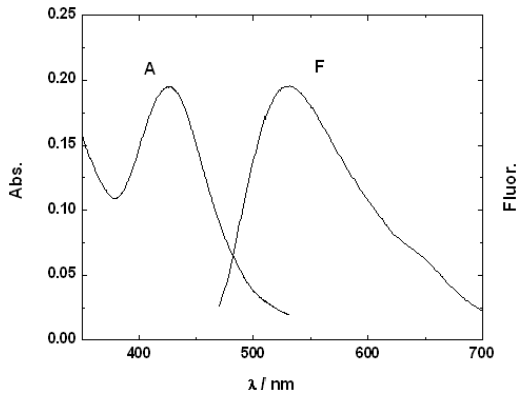

Figure 4. Absorbance (A) and fluorescence emission (F) spectra of ANNINE 5 bound to DMPC vesicles. To a suspension of vesicles containing 500 μ*M* DMPC in aqueous buffer (30 m*M* Tris, 1 m*M* EDTA, 150 m*M* NaCl, pH 7.2), 10 μ*M* ANNINE 5 (absorbance) or 0.25 μ*M* (fluorescence) were added from an ethanolic stock solution; 1.0 cm path-length quartz cuvettes were used, $T = 30°C$, bandwidths = 5 nm. The fluorescence was excited at 420 nm (+GG400 cutoff filter). The fluorescence spectrum is in arbitrary units, and its intensity has been normalized to the maximum absorbance of the absorbance spectrum.

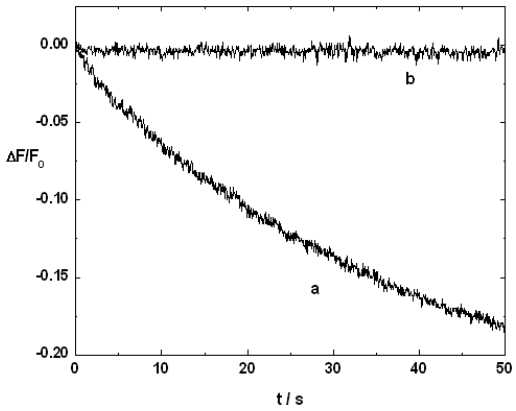

Figure 5. Relative fluorescence intensity, $\Delta F/F_0$, of ANNINE 5 as a function of time. At $t = 0$, each suspension was exposed to 436 nm light from a mercury arc lamp and the fluorescence emission was recorded at wavelengths ≥530 nm. Curve a: ANNINE 5, 0.4 μ*M*, alone in buffer; Curve b: ANNINE 5, 0.4 μ*M*, in the presence of 3 m*M* DMPC vesicles, pH = 7.2, $T = 30°C$.

minimal energy input and the twisting would likewise be expected to reverse itself on the nanosecond–picosecond time scale (43).

The fluorescence increase is, however, not unique to the lipid environment. When the dye is dissolved in chloroform, pentanol, hexanol or heptanol, a similar increase in fluorescence of the dye is observed on irradiation, although in chloroform the increase appears to follow a double-exponential time course. The increase in fluorescence is also observed when the dye is associated with SDS, DTAB or 12A9 micelles. In contrast, if the dye is dissolved in a relatively polar alcohol, such as methanol, ethanol or propanol, irradiation causes only a decrease in fluorescence over the second time scale. The fluorescence decrease is also well described by an exponential time function. It, therefore, appears that the photochemical kinetics of the dye are very dependent on the polarity of its environment. To observe an increase in fluorescence, a relatively nonpolar environment is necessary.

The fluorescence transient observed on exposure to light can be attributed to a relaxation into a new equilibrium position between the X and Y species, as described by the reaction scheme in the section describing the theory. To identify the chemical nature of the new species formed on irradiation, solutions of dye in hexanol which had undergone irradiation at 577 nm were resuspended in deuterated chloroform and analyzed by NMR spectroscopy. The spectra, however, did not show the appearance of any new peaks that would allow the identification of the new species. Therefore, it appears that the amount of product formed must be very small (<5%). The fact that it is observable at all *via* fluorescence detection is probably due to the wavelengths used, which allows a photoselection of a particular population of dye molecules, whereas NMR observes all dye molecules simultaneously.

The rate constant of the photochemical reaction responsible for the fluorescence increase in vesicles was estimated by determining the incident light intensity with the chemical potassium ferrioxalate actinometer, as described in the Materials and Methods section. The incident light intensity I_O was estimated to be $6.0(\pm 0.4) \cdot 10^{15}$ quanta s^{-1}. The average fluorescence lifetime of the dye when bound to DMPC vesicles, τ_F has been determined previously at wavelengths ≥645 nm to be 1.660 (±0.005) ns (44). By applying (Eq. 10), the fraction of RH421 in the excited state, K, can be estimated to be $1.1\ (\pm 0.4) \cdot 10^{-9}$. By applying (Eq. 7) an upper limit for the forward rate constant of the photoisomerization can be estimated from $1/\tau \geq Kk_1$. For a value of $1/\tau$ of 0.20 (±0.04) s^{-1}, measured under the same light intensity conditions as for the actinometric measurements, k_1 can, therefore, be estimated to be $\leq 1.9\ (\pm 1.1) \cdot 10^8\ s^{-1}$. This corresponds to a time constant of ≥5.3 (±3.2) ns. The observed fluorescence increase over the second time scale is, thus, entirely consistent with a very rapid photoisomerization reaction of the dye in the excited state on the nanosecond time scale. The reason the reaction is observed over a much longer time scale under constant illumination is merely that most of the dye molecules at any point in time are in the ground state rather than the excited state.

Photochemistry of ANNINE 5

In contrast to RH421, membrane-bound ANNINE 5 shows no evidence of any photochemical reaction when irradiated with light of the 436 nm mercury line. A shorter wavelength of irradiation was used for ANNINE 5 because its absorbance spectrum is significantly blueshifted in comparison to RH421. Absorbance and emission spectra of ANNINE 5 bound to DMPC vesicles are shown in Fig. 4. Although ANNINE 5 is photochemically stable when membrane bound, it does, however, undergo photobleaching in aqueous solution (see Fig. 5). The photobleaching reaction appears, however, to be inhibited when the dye is incorporated into DMPC vesicles. To avoid any photochemical reaction, it is thus essential that sufficient excess of lipid over dye is present so that all of the dye is present in the membrane phase.

To determine the lipid concentration necessary so that all of the dye is membrane bound, we have carried out a fluorescence titration of ANNINE 5 with DMPC vesicles (see Fig. 6). It was found that the following equation (based on a Langmuir adsorption isotherm) could be fitted to the data:

$$\frac{\Delta F}{F_0} = \left(\frac{\Delta F}{F_0}\right)_{\max} \cdot \frac{nK[\text{Lipid}]}{1 + nK[\text{Lipid}]} \qquad (11)$$

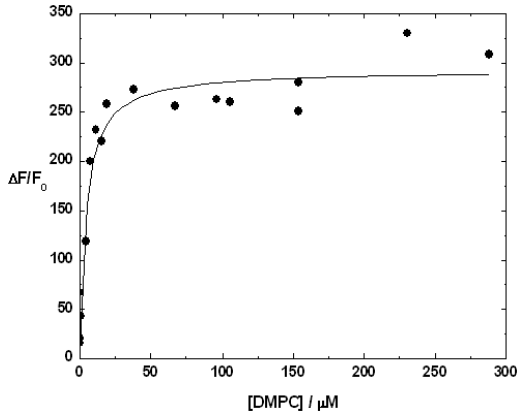

Figure 6. Fluorescence titration of ANNINE 5 (115 μ*M*) with DMPC vesicles. $\Delta F/F_0$ represents here the fluorescence intensity change on adding vesicles relative to the initial fluorescence of ANNINE 5 alone in buffer. λ_{ex} = 436 nm (+GG420 cut-off filter), λ_{em} = 550 nm (+OG530 cut-off filter), bandwidths = 10 nm, pH = 7.2, T = 30°C. The solid line represents a nonlinear least-squares fit of (Eq. 11) to the data. The values of the parameters derived were $(\Delta F/F_0)_{max}$ = 293 (±11) and nK = 2.3 (±0.5) • 10^5 M^{-1}.

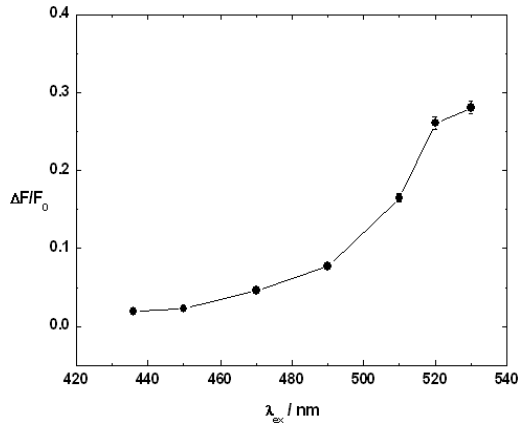

Figure 7. Relative fluorescence change, $\Delta F/F_0$, of ANNINE 5 (150 n*M*) after the addition of 1 m*M* ATP to a suspension of Na^+,K^+-ATPase-containing membrane fragments as a function of the excitation wavelength. The fluorescence emission wavelength was 550 nm (closed circles). The bandwidths used were 10 nm for both monochromators (550 nm emission). For each pair of excitation and emission wavelengths, appropriate glass cut-off filters of 10–20 nm below each wavelength were used in front of the excitation and emission monochromators to avoid any effects due to monochromator imperfections. [Na^+,K^+-ATPase] = 22 μg/mL, pH = 7.4, T = 24°C. The buffer composition was 30 m*M* imidazole, 130 m*M* NaCl, 5 m*M* $MgCl_2$ and 1 m*M* EDTA.

$\Delta F/F_0$ refers here to the relative fluorescence change after adding vesicles to the solution of dye in buffer. $(\Delta F/F_0)_{max}$ is the maximum relative fluorescence change at saturating concentrations of lipid. nK is the product of the number of dye binding sites per lipid molecule, n, and the binding constant of dye to the lipid, K. Fitting of (Eq. 11) to the data yielded the following values of the parameters: $(\Delta F/F_0)_{max}$ = 293 (±11) and nK = 2.3 (±0.5) • 10^5 M^{-1}. nK can be termed as a binding affinity of the dye for the membrane. Its reciprocal, that is, $1/(nK) = 4.4\ (\pm 1.0) \cdot 10^{-6}\ M$ or 4.4 (±1.0) μ*M*, is probably of more practical value, as this represents the lipid concentration necessary for 50% binding of the dye. The value of nK can be compared to the corresponding value for RH421 binding to DMPC vesicles, which has previously been determined (32) to be 5.2 (±0.5) • 10^4 M^{-1}, that is $1/(nK)$ = 19 (±2) μ*M*. ANNINE 5 thus has a significantly higher binding affinity to lipid membranes than RH421, most likely because of its more extended hydrophobic aromatic system.

As with other dyes of this class, the incorporation of ANNINE 5 into the membrane is a relatively slow process, occurring over the minute time scale. Stopped-flow kinetic studies, which have previously been undertaken with RH421, showed that this is due to the formation of large dye aggregates in the aqueous phase, which must disaggregate before dye incorporation into the membrane occurs (34). The rate-determining step was found to be the disaggregation of the aggregates into dye monomers rather than the subsequent binding of a monomer to the membrane. The incorporation of ANNINE 5 into the membrane was found to be even slower than RH421, probably also due to its more extended aromatic system. Incorporation of ANNINE 5 into the membrane requires an equilibration time of at least 15 min.

Na^+,K^+-ATPase sensitivity of RH421 and ANNINE 5

RH421 has already been successfully used to probe changes in local intramembrane electrical field strength due to reactions of the Na^+,K^+-ATPase, in particular the reactions triggered by its phosphorylation by ATP (13–17) but also reactions involving ion binding (45–48). Up to now, however, no studies using ANNINE 5 have been reported. Therefore the responses of RH421 and ANNINE 5 are compared here. Because ATP phosphorylation of membrane-bound RH421 causes a redshift of the dye's excitation spectrum, it has been shown that the maximum relative fluorescence changes, $\Delta F/F_0$, that is, the maximum dye sensitivity, is found when the dye is excited on the red edge of its excitation spectrum (39). Normally an excitation wavelength of 570 nm is used. Similar behavior has been found by Kuhn and Fromherz (26) for ANNINE dyes when an external electric field was applied to stained HEK cells.

For the Na^+,K^+-ATPase preparation used in this study, the relative fluorescence change of RH421, $\Delta F/F_0$, after ATP addition under the conditions described in the Materials and Methods section was 0.31 (±0.01). For this measurement the wavelengths used were λ_{ex} = 570 nm (+OG530 cut-off filter) and λ_{em} = 670 nm (+RG645 cut-off filter) and the bandwidths of both the excitation and emission monochromators were set at 10 nm. With the use of the same Na^+,K^+-ATPase preparation, experiments were also performed in which RH421 was substituted by ANNINE 5. In this case, measurements were carried out over a range of excitation wavelengths, from 436 to 530 nm (see Fig. 7). The emission wavelength was at 550 nm. It can be seen that $\Delta F/F_0$ increases significantly as the excitation wavelength increases, from 0.019 (±0.001) at 436 nm excitation up to 0.28 (±0.01). This is consistent with the finding of Kuhn and Fromherz (26) of an enhancement of the voltage sensitivity of the ANNINE dyes on long-wavelength excitation when tested on cultured HEK cells. The reason for the increased sensitivity on long-wavelength excitation is simply that changes in intramembrane electric field strength cause a wavelength shift of the dye's absorbance spectrum. Higher relative changes in fluorescence thus occur when exciting on the flanks of the absorbance spectrum, where the relative changes in absorbance are also higher (26,39). At the longest excitation wavelength, 530 nm, the magnitude of $\Delta F/F_0$ obtained with the use of ANNINE 5 is comparable to that obtained

with RH421. Both dyes thus appear to be equally suitable for studies of Na^+,K^+-ATPase function, at least as long as kinetic resolution of the enzyme's partial reactions is not required.

DISCUSSION

The photochemical behavior of the voltage-sensitive dyes RH421 and ANNINE 5 when bound to dimyristoylphosphatidylcholine vesicles has been investigated. Whereas RH421 displays a fluorescence increase on continuous illumination, which occurs over the second time scale, ANNINE 5 yielded a constant fluorescence level, as long as all the dye is bound to the membrane phase. ANNINE 5, thus, has the significant advantage over RH421 that it is photochemically more stable. The greater stability arises presumably from the more rigid ring structure of ANNINE 5 (see Fig. 1). RH421, on the other hand, has two *trans* double bonds between the anilino and pyridinium rings, which would be susceptible to *trans* → *cis* photoisomerization.

Although the photochemical reaction of membrane-bound RH421 occurs over the second time scale (see Fig. 2), it is in fact due to a reaction occurring in the excited state in the nanosecond time scale. This has been shown here by measuring the intensity of the exciting light and calculating the relative number of dye molecules in the excited and ground states. The relatively slow photochemical kinetics of RH421 observed under constant illumination is simply due to the fact that the vast majority of dye molecules at any point in time are in the ground state. Time-resolved fluorescence lifetime measurements of RH421 bound to DMPC vesicles (33,49,50) have already shown that the dye undergoes an excited-state reaction in which a new fluorescent species is produced. The time constant of the reaction was determined to be 100–200 ps (33), corresponding to a rate constant of $1–2 \cdot 10^{10}$ s^{-1}. This reaction is approximately two orders of magnitude faster than the reaction observed here under conditions of constant illumination, but the two reactions could possibly be sequential reactions along a reaction mechanism leading to the same final product. The excited-state reaction observed in the time-resolved fluorescence lifetime studies was previously attributed (50) to the formation of a fluorescent twisted intramolecular charge transfer (TICT) state, occurring simultaneously with the relaxation of the surrounding solvent cage. Because the reaction observed in this study under constant illumination is irreversible on the time scale of the measurement when the reaction mixture is in the dark, a new stable ground-state species must also be formed. It is, therefore, very likely that the excited-state reaction does not stop at the formation of a TICT state and reorganization of the solvent cage, but proceeds further along the pathway to the formation of a new isomer; that is, most likely a *cis* isomer is formed from the original *trans* state.

This interpretation is also supported by the results of Ephardt and Fromherz (19), who showed that the quantum yield, ϕ_{TC}, for *trans* → *cis* photoisomerization of a very similar styrylpyridinium dye (dibutylaminostilbazolium butylsulphonate) is very dependent on the polarity of the solvent. In water, a very polar solvent, they determined a ϕ_{TC} value of 0.002, whereas in chloroform, a much less polar solvent, they determined a ϕ_{TC} of 0.13, that is, an increase in the quantum yield of almost two orders of magnitude. In contrast, they found that the quantum yield for the reverse process, *cis* → *trans* photoisomerization was virtually independent of the polarity of the solvent. The reaction of RH421 observed here was found to be very dependent on solvent polarity. An increase in fluorescence on irradiation was only observed in solvents of relatively low polarity, that is, chloroform, pentanol, hexanol, heptanol and when bound to vesicles or micelles. Based on the results of Ephardt and Fromherz (19), this would, therefore, suggest that the reaction occurring is likely to be a *trans* → *cis* photoisomerization. Ephardt and Fromherz found furthermore that the increase in quantum yield for *trans* → *cis* photoisomerization correlated with an increase in the fluorescence quantum yield. They then suggested that the increased *trans* → *cis* photoisomerization quantum yield could be explained by a decrease in the efficiency of a competing radiationless deactivation process. For the excited-state photoisomerization reaction they estimated a rate constant of $1.2 \cdot 10^{10}$ s^{-1}. This is in very good agreement with the rate constant of $1–2 \cdot 10^{10}$ s^{-1} determined by Zouni *et al.* (33) for the excited-state reaction of RH421 bound to DMPC vesicles from fluorescence lifetime measurements. The somewhat lower rate constant found here from photostationary studies, which detect the formation of a new *ground*-state species, could be accounted for by further rate-limiting reactions on the pathway to a ground-state *cis* isomer.

The fact that ANNINE 5 is much more stable photochemically than RH421 suggests that it may be a more reliable voltage-sensitive probe for studying ion-transporting membrane proteins. The experiments performed here indicate that it indeed has a similar sensitivity to RH421 to changes in local electric field strength, at least in Na^+,K^+-ATPase membrane fragments, as long as it is excited on the far red edge of its absorbance spectrum, that is, 530 nm. For rapid kinetic measurements, in which only a small time is available for fluorescence averaging, it is necessary to use an intense light source, such as a mercury arc lamp or a laser. Unfortunately, the polycyclic ring structure of ANNINE 5 shifts its longest-wavelength UV/visible absorbance band to the blue relative to RH421, into a region where no significant mercury lines are available for excitation. Because mercury lamps are the most routinely used light sources for stopped-flow fluorescence studies, this is a current limitation to the applicability of ANNINE 5. At present we are therefore investigating the possibility of aliphatic bridges to the *trans* double bonds of RH421, as these would be predicted also to inhibit any photochemical reactions but without any significant perturbation to the dye's conjugated system.

Acknowledgements—We thank Professor Dr. Peter Fromherz for the kind gift of the dye ANNINE 5, Dr. Marlon Hinner for helpful discussions, and Milena Roudna for expert technical assistance. R.J.C. and P.S. acknowledge financial support from the Australian Research Council (Linkage International Award LX0454408) and from the Australian Research Council/National Health and Medical Research Council funded Research Network "Fluorescence Applications in Biotechnology and Life Sciences" (RN0460002).

REFERENCES

1. Grinvald, A., R. Hildesheim, I. C. Farber and L. Anglister (1982) Improved fluorescent probes for the measurement of rapid changes in membrane potential. *Biophys. J.* **39**, 301–308.
2. Grinvald, A., A. Fine, I. C. Farber and R. Hildesheim (1983) Fluorescence monitoring of electrical responses from small neurons and their processes. *Biophys. J.* **42**, 195–198.
3. Hassner, A., D. Birnbaum and L. M. Loew (1984) Charge-shift probes of membrane potential. Synthesis. *J. Org. Chem.* **49**, 2546–2551.
4. Fluhler, E., V. G. Burnham and L. M. Loew (1985) Spectra, membrane binding, and potentiometric responses of new charge shift probes. *Biochemistry* **24**, 5749–5755.

5. Bedlack, R. S., Jr., M. D. Wei and L. M. Loew (1992) Localized membrane depolarizations and localized calcium influx during electric field-guided neurite growth. *Neuron* **9**, 393–403.
6. Bedlack, R. S., Jr., M. D. Wei, S. H. Fox, E. Gross and L. M. Loew (1994) Distinct electrical potentials in soma and neurite membranes. *Neuron* **13**, 1187–1193.
7. Zhang, J., R. M. Davidson, M. D. Wei and L. M. Loew (1998) Membrane electric properties by combined patch clamp and fluorescence ratio imaging in single neurons. *Biophys. J.* **74**, 48–53.
8. Grinvald, A., R. D. Frostig, E. Lieke and R. Hildesheim (1988) Optical imaging of neuronal activity. *Physiol. Rev.* **68**, 1285–1366.
9. Loew, L. M. (1994) Voltage-sensitive dyes and imaging neuronal activity. *Neuroprotocols* **5**, 72–79.
10. Fromherz, P. and C. O. Müller (1994) Cable properties of a straight neurite of a leech neuron probed by a voltage-sensitive dye. *Proc. Natl. Acad. Sci. U S A* **91**, 4604–4608.
11. Gogan, P., I. Schmiedel-Jakob, Y. Chitti and S. Tyč-Dumont (1995) Fluorescence imaging of local membrane electric fields during the excitation of single neurons in culture. *Biophys. J.* **69**, 299–310.
12. Canepari, M., M. Campani, L. Spadavecchia and V. Torre (1996) CCD imaging of the electrical activity in the leech nervous system. *Eur. Biophys. J.* **24**, 359–370.
13. Klodos, I. and B. Forbush III. (1988) Rapid conformational changes of the Na/K pump revealed by a fluorescent dye. *J. Gen. Physiol.* **92**, 46a.
14. Pratap, P. R. and J. D. Robinson (1993) Rapid kinetic analyses of the Na^+/K^+-ATPase distinguish among different criteria for conformational change. *Biochim. Biophys. Acta* **1151**, 89–98.
15. Heyse, S., I. Wuddel, H. J. Apell and W. Stürmer (1994) Partial reactions of the Na,K-ATPase: determination of rate constants. *J. Gen. Physiol.* **104**, 197–240.
16. Kane, D. J., K. Fendler, E. Grell, E. Bamberg, K. Taniguchi, J. P. Froehlich and R. J. Clarke (1997) Stopped-flow kinetic investigations of conformational changes of pig kidney Na^+,K^+-ATPase. *Biochemistry* **36**, 13406–13420.
17. Cornelius, F., N. U. Fedosova and I. Klodos (1998) E_2P phosphoforms of Na,K-ATPase. II. Interaction of substrate and cation-binding sites in P_i phosphorylation of Na,K-ATPase. *Biochemistry* **37**, 16686–16696.
18. Schaffer, P., H. Ahammer, W. Müller, B. Koidl and H. Windisch (1994) Di-4-ANEPPS causes photodynamic damage to isolated cardiomyocytes. *Pflügers Arch.* **426**, 548–551.
19. Ephardt, H. and P. Fromherz (1989) Fluorescence and photoisomerization of an amphiphilic aminostilbazolium dye as controlled by the sensitivity of radiationless deactivation to polarity and viscosity. *J. Phys. Chem.* **93**, 7717–7725.
20. Heberle, J. and N. A. Dencher (1992) Surface-bound optical probes monitor proton translocation and surface potential changes during the bacteriorhodopsin photocycle. *Proc. Natl. Acad. Sci. U S A* **89**, 5996–6000.
21. Peinelt, C. and H. J. Apell (2003) Time-resolved partial reactions of the SR Ca-ATPase investigated with a fluorescent styryl dye. *Ann. N. Y. Acad. Sci.* **986**, 325–326.
22. Frank, J., A. Zouni, A. van Hoek, A. J. W. G. Visser and R. J. Clarke (1996) Interaction of the fluorescent probe RH421 with ribulose-1,5-bisphosphate carboxylase/oxygenase and with Na^+,K^+-ATPase membrane fragments. *Biochim. Biophys. Acta* **1280**, 51–64.
23. Deguchi, N., P. L. Jørgensen and A. B. Maunsbach (1977) Ultrastructure of the sodium pump. Comparison of thin sectioning, negative staining, and freeze-fracture of purified, membrane-bound (Na^+,K^+)-ATPase. *J. Cell Biol.* **75**, 619–634.
24. Pedersen, M., M. Roudna, S. Beutner, M. Birmes, B. Reifers, H. D. Martin and H. J. Apell (2002) Detection of charge movements in ion pumps by a family of styryl dyes. *J. Membr. Biol.* **185**, 221–236.
25. Hübener, G., A. Lambacher and P. Fromherz (2003) Anellated hemicyanine dyes with large symmetrical solvatochromism of absorption and fluorescence. *J. Phys. Chem. B* **107**, 7896–7902.
26. Kuhn, B. and P. Fromherz (2003) Anellated hemicyanine dyes in a neuron membrane: molecular Stark effect and optical voltage recording. *J. Phys. Chem. B* **107**, 7903–7913.
27. Kuhn, B., P. Fromherz and W. Denk (2004) High sensitivity of Stark-shift voltage-sensing dyes by one- or two-photon excitation near the red spectral edge. *Biophys. J.* **87**, 631–639.
28. Jørgensen, P. L. (1974) Purification and characterization of $(Na^+ + K^+)$-ATPase III. Purification from the outer medulla of mammalian kidney after selective removal of membrane components by sodium dodecylsulphate. *Biochim. Biophys. Acta* **356**, 36–52.
29. Jørgensen, P. L. (1974) Isolation of $(Na^+ + K^+)$-ATPase. *Methods Enzymol.* **32**, 277–290.
30. Schwartz, A., K. Nagano, M. Nakao, G. E. Lindenmayer, J. C. Allen and H. Matsui (1971) The sodium- and potassium-activated adenosinetriphosphatase. *Methods Pharmacol.* **1**, 361–388.
31. Lowry, O. H., N. J. Rosebrough, A. L. Farr and R. J. Randall (1951) Protein measurement with the Folin phenol reagent. *J. Biol. Chem.* **193**, 265–275.
32. Jørgensen, P. L. and J. P. Andersen (1988) Structural basis for E_1–E_2 conformational transitions in Na,K-pump. *J. Membr. Biol.* **103**, 95–120.
33. Zouni, A., R. J. Clarke, A. J. W. G. Visser, N. V. Visser and J. F. Holzwarth (1993) Static and dynamic studies of the potential-sensitive membrane probe RH421 in dimyristoylphosphatidylcholine vesicles. *Biochim. Biophys. Acta* **1153**, 203–212.
34. Zouni, A., R. J. Clarke and J. F. Holzwarth (1994) Kinetics of solubilization of styryl dye aggregates by lipid vesicles. *J. Phys. Chem.* **98**, 1732–1738.
35. Hatchard, C. G. and C. A. Parker (1956) A new sensitive chemical actinometer. II. Potassium ferrioxalate as a standard chemical actinometer. *Proc. R. Soc. London Ser. A* **235**, 518–536.
36. Demas, J. N., W. D. Bowman, E. F. Zalewski and R. A. Velapoldi (1981) Determination of the quantum yield of the ferrioxalate actinometer with electrically calibrated radiometers. *J. Phys. Chem.* **85**, 2766–2771.
37. Parker, C. A. (1968) *Photoluminescence of Solutions*, pp. 208–214. Elsevier, Amsterdam.
38. Cevc, G. (1993) Thermodynamic parameters of phospholipids. In *Phospholipid Handbook* (Edited by G. Cevc), pp. 939–956. Marcel Dekker, New York.
39. Bühler, R., W. Stürmer, H. J. Apell and P. Läuger (1991) Charge translocation by the Na,K-pump: I. Kinetics of local field changes studied by time-resolved fluorescence measurements. *J. Membr. Biol.* **121**, 141–161.
40. Steiner, U., M. H. Abdel-Kader, P. Fischer and H. E. A. Kramer (1978) Photochemical *cis/trans* isomerization of a stilbazolium betaine. A protolytic/photochemical reaction cycle. *J. Am. Chem. Soc.* **100**, 3190–3197.
41. Görner, H. and D. Schulte-Frohlinde (1985) The role of triplet states in the *trans* → *cis* photoisomerization of quaternary salts of 4-nitro-4′-azastilbene and their quinolinium analogues. 6. *J. Phys. Chem.* **89**, 4105–4112.
42. Struve, W. S., P. M. Rentzepis and J. Jortner (1973) Solvent reorganization around a ''giant dipole'' molecule. *J. Chem. Phys.* **59**, 5014–5019.
43. Strehmel, B. and W. Rettig (1996) Photophysical properties of fluorescence probes I: dialkylamino silbazolium dyes. *J. Biomed. Opt.* **1**, 98–109.
44. Visser, N. V., A. van Hoek, A. J. W. G. Visser, J. Frank, H. J. Apell and R. J. Clarke (1995) Time-resolved fluorescence investigations of the interaction of the voltage-sensitive probe RH421 with lipid membranes and proteins. *Biochemistry* **34**, 11777–11784.
45. Fedosova, N. U. and I. Klodos (1994) Conformational states of Na^+/K^+-ATPase probed with RH421 and eosin. In *The Sodium Pump: Structure Mechanism, Hormonal Control and Its Role in Disease* (Edited by E. Bamberg and W. Schoner), pp. 561–564, Steinkopff Verlag, Darmstadt.
46. Ruf, H., E. Lewitzki and E. Grell (1994) Na^+/K^+-ATPase: Probing for a high affinity binding site for Na^+ by spectrofluorometry. In: *The Sodium Pump: Structure Mechanism, Hormonal Control and Its Role in Disease* (Edited by E. Bamberg and W. Schoner), pp. 569–572. Steinkopff Verlag, Darmstadt.
47. Schneeberger, A. and H. J. Apell (2001) Ion selectivity of the cytoplasmic binding sites of the Na,K-ATPase: II. Competition of various cations. *J. Membr. Biol.* **179**, 263–273.
48. Humphrey, P. A., C. Lüpfert, H. J. Apell, F. Cornelius and R. J. Clarke (2002) Mechanism of the rate-determining step of the Na^+,K^+-ATPase pump cycle. *Biochemistry* **41**, 9496–9507.
49. Visser, N. V., A. van Hoek, A. J. W. G. Visser, J. Frank, H. J. Apell and R. J. Clarke (1995) Time-resolved fluorescence investigations of the interaction of the voltage-sensitive probe RH421 with lipid membranes and proteins. *Biochemistry* **34**, 11777–11784.
50. Visser, N. V., A. van Hoek, A. J. W. G. Visser, R. J. Clarke and J. F. Holzwarth (1994) Time-resolved polarized fluorescence of the potential-sensitive dye RH421 in organic solvents and micelles. *Chem. Phys. Lett.* **231**, 551–560.